ACS APPLIED MATERIALS & INTERFACES

Research Article

www.acsami.org

Fabrication of Antireflective Compound Eyes by Imprinting

Feifei Wu, Gang Shi, Hongbo Xu, Lingxiao Liu, Yandong Wang, Dianpeng Qi, and Nan Lu*

State Key Laboratory of Supramolecular Structure and Materials, College of Chemistry, Jilin University, Changchun 130012, P. R. China

Supporting Information

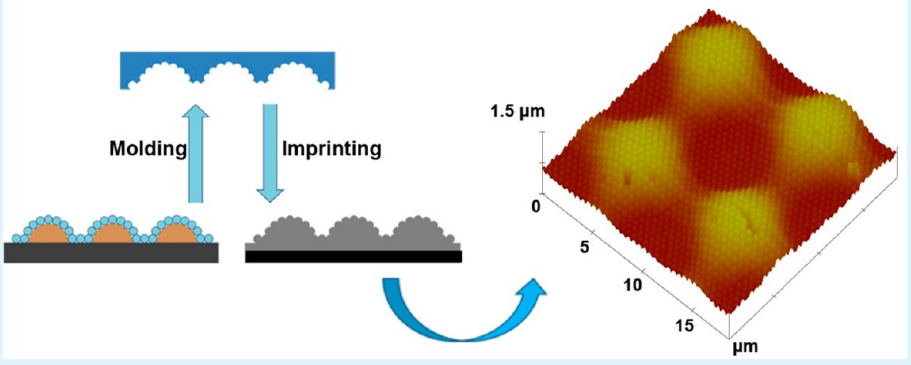

ABSTRACT: In this article, we demonstrate a simple and cost-effective approach to fabricate antireflective polymer coatings. The antireflective surfaces have 3D structures that mimick moth compound eyes. The fabrication is easily performed via a one-step imprinting process. The 3D arrays exhibit better antireflective performance than 2D arrays over most wavelengths from 400 to 2400 nm. The reflectivity of the 3D arrays is lower than 5.7% over the all of the wavelengths, and the minimum reflectivity is 0.27% at a wavelength of around 1000 nm.

KEYWORDS: *nanoimprint lithography, hierarchical structures, antireflection, moth eyes, assembling*

INTRODUCTION

Surfaces with hierarchical structures have attracted great attention because of their unique optical properties and promising applications in solar cells, light sensors, LEDs, and optical devices.[1−5] These properties have fascinated many research groups, prompting their thorough investigation. The moth eye is one of the most prominent examples, whose nipple arrays on the corneal surfaces can suppress reflection significantly.[6] So far, many fabricating approaches have been developed to mimic the moth eye structure, including electron-beam lithography (EBL), laser interference lithography (LIL), reactive-ion etching (RIE), phase separation, and so on.[7−14] However, most of these approaches are restricted by their complicated serial treating processes and expensive instruments. To overcome these limitations, many template methods (e.g., colloidal lithography,[15,16] soft lithography,[17−19] lithographically controlled wetting,[20] and nanoembedding[21]) have been proposed to fabricate antireflective hierarchical structures at a low cost and with a large area. Generally, it is difficult to obtain hierarchical structures via one technique. Most techniques need to be combined with other techniques, which introduces serial steps and complicates the fabrication process. Recently, imprinting methods have been reported to fabricate hierarchical structures on a large area.[22] Usually, to fabricate hierarchical structures using a 2D mold involves multistep imprinting, which requires more time and introduces more defects to the structures. Therefore, developing a new method with one step to fabricate 3D antireflective structures is necessary.

Herein, we present a simple and cost-effective method to fabricate antireflective surfaces by mimicking the hierarchical structures on moth eyes. The 3D antireflective stamp was obtained by a replica molding technique, and the antireflective polymer surface was directly obtained via one-step imprinting. The obtained 3D arrays exhibit better antireflective performance than 2D arrays over most wavelengths from 400 to 2400 nm, which could be used for improving the performance of optical devices.

EXPERIMENTAL SECTION

Materials. The monodispersed 580 nm polystyrene (PS) spheres with a concentration of 10 wt % were purchased from Sigma-Aldrich. Positive photoresist BP212 and its developer were purchased from Beijing Institute of Chemical Reagents. Ethanol, acetone, chloroform, and dodecylsodiumsulfate (SDS) were obtained from commercial sources in the highest available purity. Ultrapure water (18.2 MΩ cm) was used (Millipore System, Marlborough, France). The silicon wafers [n type (100)] (Youyan Guigu, Beijing, China) and glass slices were used for substrates. A kit of a prepolymer of Sylgard 184 polydimethylsiloxane (PDMS, Dow Corning Corporation) was used

Received: January 25, 2013
Accepted: December 2, 2013
Published: December 2, 2013

for replica molding. Norland Optical Adhesive 63 (NOA-63, Norland Products Inc.) was used for preparing the antireflective coatings.

Substrate Preparation. Silicon slices (approximately 2 × 2 cm^2) were treated with an oxygen plasma system (100, PVA Tepla) at 300 W and 660 mTorr for 3 min and were then cleaned with acetone, chloroform, and ethanol in an ultrasonic bath for 3 min. Then, the substrates were rinsed with deionized water and dried under a nitrogen gas flow. A spin-coating procedure (3000 rpm for 30 s) was used to form a photoresist (BP212) layer on the substrate following by baking at 88 °C for 30 min. Then, the photoresist (BP212) layer was treated with photolithography (UV at 1000 W for 1 min). After a heating treatment at 120 °C for 30 min, the obtained photoresist (BP212) patterns were changed to hemispheres. Finally, the substrate was immersed in a 10% SDS solution and kept there for 10 min.

Fabrication of the 3D Hierarchical Stamp. The monolayer of PS spheres was prepared as described elsewhere.[23−25] By lifting the substrate from the water surface, the highly ordered PS monolayer was transferred onto the prepatterned substrate. Then, the PS sphere monolayer on the prepatterned substrate was employed as a template for producing the 3D PDMS stamp by a molding technique, and the 3D PDMS stamp was used for UV-imprinting lithography (UV-NIL).

Fabrication of the Compound Eyes Arrays. To achieve the compound eyes arrays, a NOA-63 layer with 500 nm thickness was prepared by spin-coating on glass slice, and a UV-NIL process was performed on the commercial UV-NIL equipment (Obducat AB, Malmö, Sweden) with the 3D PDMS stamp. In the UV-NIL process, a pressure of 15 bar was employed for 2 min at room temperature.

Measurements. A nanoscope scanning probe microscope (Dimension 3100, Digital Instruments, Santa Barbara, CA) was used for collecting atomic force microscope (AFM) images under ambient conditions. The spring constant of silicon cantilevers (Nanosensors, Digital Instruments) was 250−350 kHz. UV−vis reflection spectra were recorded using a spectrophotometer (Shimadzu UV3600, Shimadzu, Japan). The surface morphology of the 3D arrays was characterized using a field-emission scanning electron microscope (SEM, JSM 6700F, JEOL, Japan) with an electron energy of 3 kV. To improve conductivity, a layer of Pt (ca. 2 nm in thickness) was sputtered on the samples.

RESULTS AND DISCUSSION

The procedure for fabricating artificial moth compound eyes is outlined in Figure 1A. To produce a micropatterned surface, a layer of photoresist (BP212) was initially spin-coated on the silicon substrate, and photolithography was applied to introduce the micropattern arrays. The micropattern comprises 5 μm squares with a height of 1 μm separated by 5 μm spacing. For minimizing the interfacial energy,[26] the photoresist squares were changed to microhemispheres by a heating treatment at 120 °C for 30 min (Figure 1A-a). Then, the microhemisphere-patterned surface was used as a substrate for assembling PS spheres. A monolayer of hexagonal close-packed PS spheres with 580 nm diameter was formed on the microhemisphere-

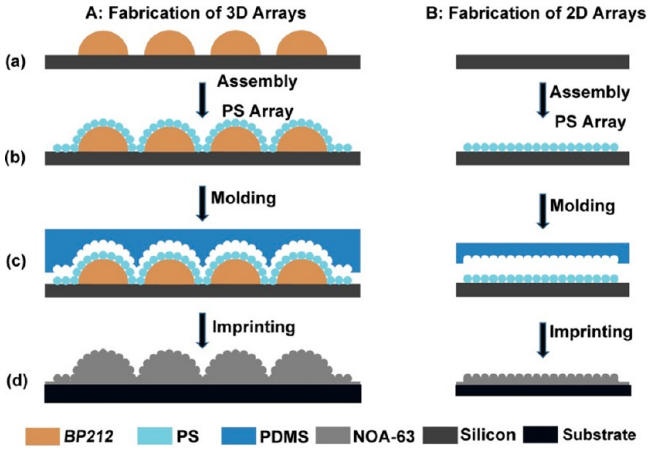

Figure 1. Scheme of the procedure for creating biomimetic antireflective (A) 3D arrays and (B) 2D arrays. (a) Preparation of substrate, (b) assembly of PS arrays on the substrate, (c) replica molding of PS arrays assembled on the substrate, and (d) imprinting using the replica mold and the lift-off of the mold after imprinting.

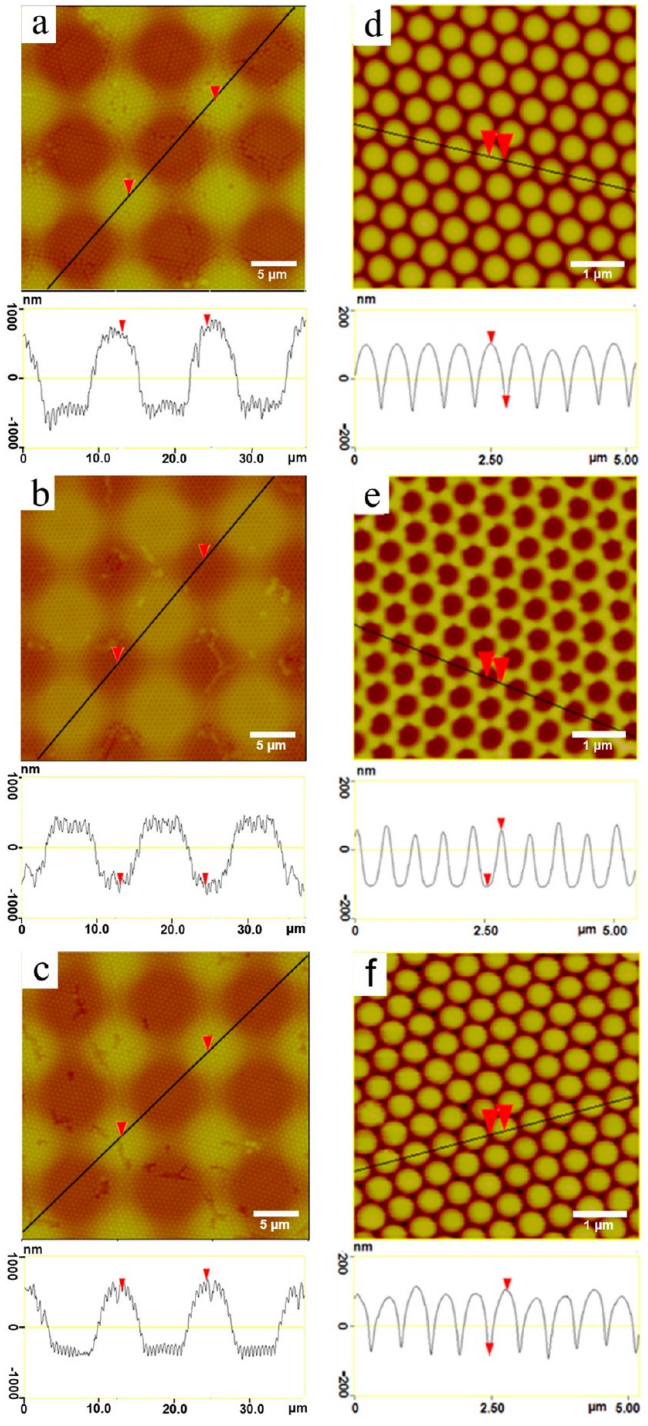

Figure 2. AFM image of (a) the PS spheres monolayer assembled on the prepatterned substrate, (b) 3D PDMS stamp molded from panel a, (c) imprinted NOA-63 arrays with panel b, (d) PS spheres monolayer assembled on flat silicon, (e) 2D PDMS molded from panel d, and (f) imprinted NOA-63 arrays with panel e.

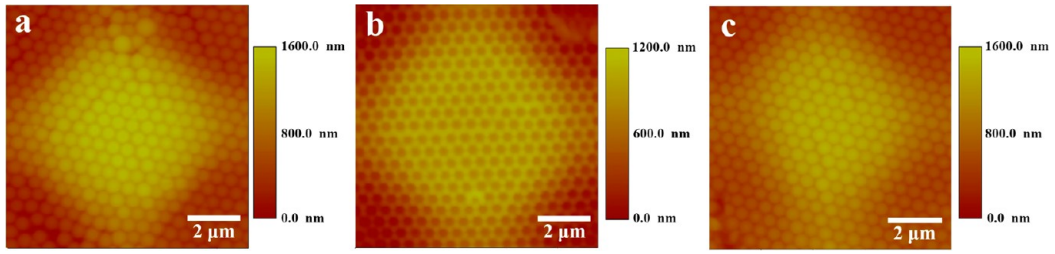

Figure 3. (a–c) Enlarged AFM images corresponding to Figure 2, panels a, b, and c, respectively.

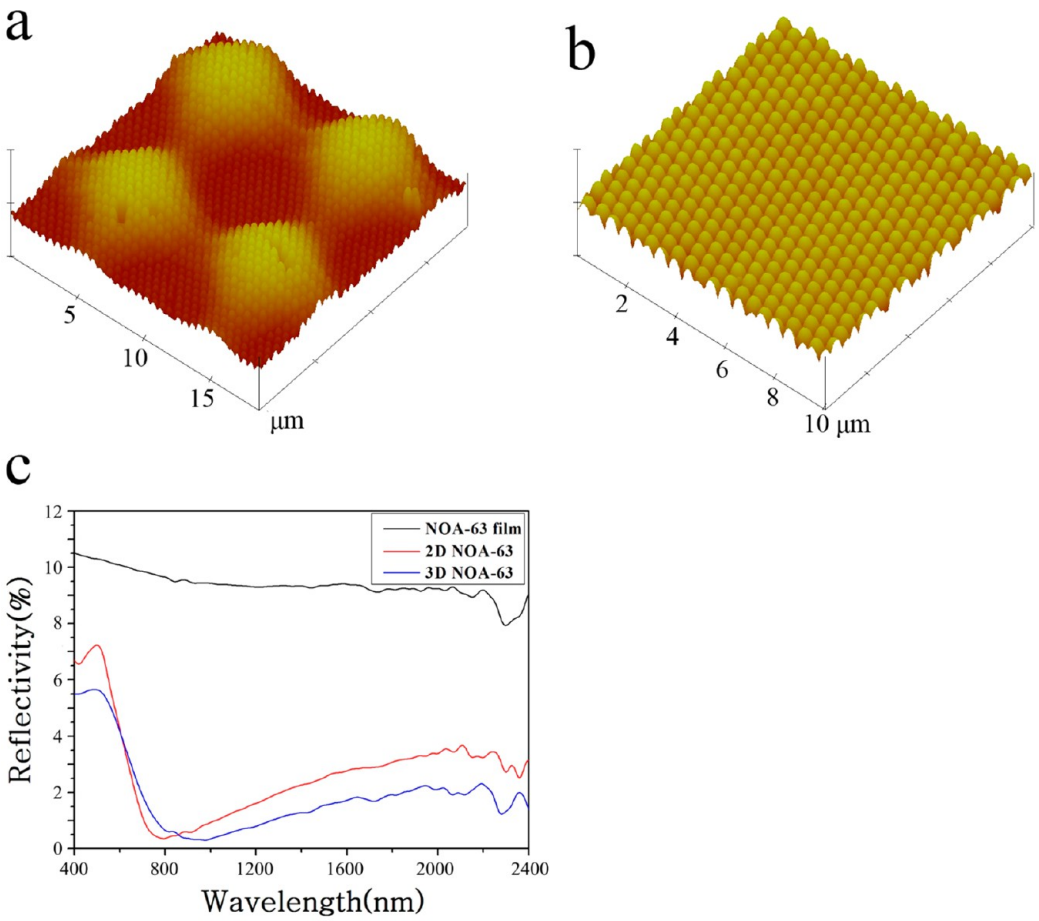

Figure 4. Three-dimensional AFM images of the imprinted (a) 3D and (b) 2D NOA-63 arrays and (c) hemispherical reflection for a flat NOA-63 film (black line), 2D arrays (red line), and an artificial compound eyes array (blue line) at normal incidence.

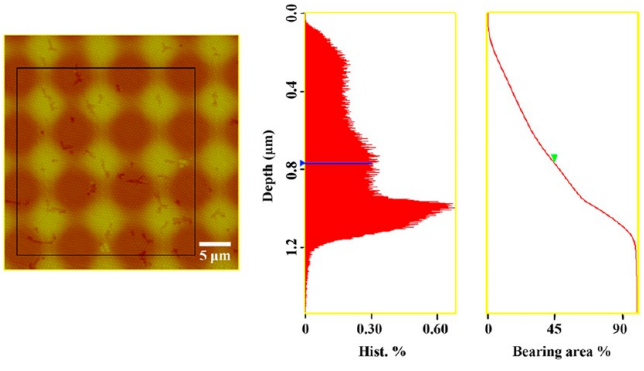

Figure 5. Bearing analysis of the fabricated hierarchical array.

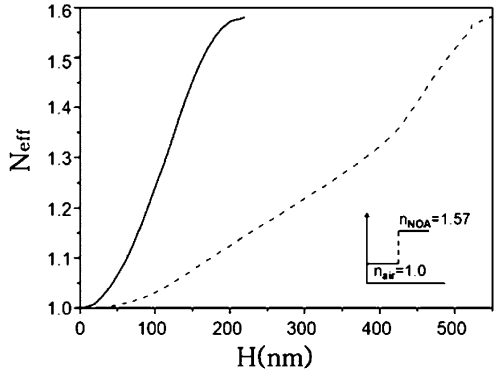

Figure 6. Correlation of n_{eff} and H of the 3D NOA-63 arrays (dashed line) and 2D NOA-63 arrays (solid line). The inset shows the refractive index of a flat NOA-63 film for reference.

patterned surface (Figure1A-b). Subsequently, for replicating the biomimetic structure efficiently, a PDMS stamp was

fabricated via molding the 3D hierarchical arrays (Figure 1A-c). Finally, a UV-NIL process was carried out with the 3D PDMS stamp to create the 3D NOA-63 arrays (Figure 1A-d). For comparison, 2D arrays were fabricated with a similar method, and the procedure is shown in Figure 1B. The microhemispheres covered by the assembled 580 nm spheres are shown in Figure 2a. Remarkably, the morphology of the fabricated structures is similar to the structures of natural moth eyes. As revealed in Figure 2b, the structure of PDMS is the reverse of the 3D hierarchical arrays. Figure 2b reveals that the stamp was copied perfectly from the 3D hierarchical arrays. Figure 2c shows the AFM image of the NOA-63 with compound eyes arrays, which is a replica of the structure in Figure 2a. The enlarged AFM images of Figure 2a−c are given in Figure 3, which reveal that the pattern of the PS spheres are clear in the 3D arrays. AFM images of the 2D PS sphere arrays, 2D PDMS stamp, and imprinted 2D NOA-63 arrays are presented in Figure 2d−f, respectively. Similarly, the height and period of the 2D NOA-63 arrays are consistent with that of the primary mold in Figure 2d (580 nm). Because of the intrinsic limits of AFM, SEM images of large-area 3D arrays were collected and are shown in Figure S1 (Supporting Information). Figure 4a,b presents the 3D AFM images of the 3D NOA-63 arrays and 2D NOA-63 arrays, respectively.

The hemispherical reflectivity of the artificial compound eyes arrays was evaluated using visible-near-infrared radiation reflectivity measurement at an incidence angle of 5°. Figure 4c presents the reflectivity of a flat NOA-63 film (black line), 2D NOA-63 arrays (red line), and 3D NOA-63 with biomimetic moth eyes arrays (blue line). The flat NOA-63 film (black line) exhibits a high reflectivity (about 10%) for visible and near-infrared wavelengths. The reflectivity of the 2D arrays is lower than 7.5% from 400 to 2400 nm, and the lowest reflectivity of around 0.3% is observed at 800 nm. For the artificial compound eyes (blue line), the reflectivity is lower than 5.7% at wavelengths from 400 to 2400 nm, and the minimal reflectivity can even be reduced to 0.27% at a wavelength of around 1000 nm. We found that the wavelength of the minimum reflectivity for the structure with a larger period has a red shift, as reported in the literature.[27] Therefore, the antireflective performance of 3D arrays is less than that of 2D arrays between 600 and 850 nm. However, compared with 2D arrays, the reflectivity of 3D arrays is reduced by 18 and 40% for wavelengths ranging from 400 to 600 nm and from 850 to 2400 nm, respectively. The antireflective performance of 3D arrays is better than that of 2D arrays over most wavelengths.

On the basis of the effective medium theory,[28,29] the antireflective arrays (ARs) can be considered to be an inserted layer with an effective refraction index, n_{eff}. For ideal ARs with near zero reflectivity, the n_{eff} value should increase gradually from 1 to n_{sub} from the interface of the air/ARs to the interface of the ARs/substrate. The effective refractive index for normal incidence can be written as

$$n_{eff} = \sqrt{n_1^2 f + n_2^2 (1 - f)} \quad (1)$$

where n_1 is the refractive index of air, n_2 is the refractive index of the polymerized NOA-63 structure, and f is the fill factor of the antireflective arrays.[30−32] A theoretical simulation of the effective refractive index profiles was introduced to interpret the antireflective properties of different NOA-63 morphologies.[24,33] According to the definition, the value of f can be considered as the area ratio from bearing analysis of the AFM image given in Figure 5. The area ratio depends on the height (H) of the antireflective arrays, so the value of f of different antireflective arrays can be obtained according to their heights.

The correlation of n_{eff} and H was calculated and is plotted in Figure 6. The n_{eff} value changes abruptly from 1.0 to 1.57 across the air/NOA-63 interface (inset of Figure 6), resulting in a high reflection of the flat NOA-63 film substrate. To reduce the reflection, the n_{eff} should be changed gradually. For 2D (solid line in Figure 6) and 3D arrays (dashed line in Figure 6), the n_{eff} value changes continuously from 1.0 to 1.57, so 2D arrays and 3D arrays exhibit a lower reflectivity than the flat-film substrate. The height of the 3D arrays is higher than that of the 2D arrays, which results in a much more gradual change of n_{eff} compared to that of the 2D arrays. With the same variation of n_{eff}, 3D arrays provide a smaller slope than the 2D arrays, which makes the 3D arrays exhibit a lower reflectivity. Hence, 3D arrays exhibit better antireflective performance.

CONCLUSIONS

We present a simple approach for the preparation of a hierarchical polymer structure to mimic moth compound eyes. The hierarchical polymer structure is fabricated by a one-step imprinting process, with the stamp fabricated by easily molding the prepared micro- and nanostructures. The 3D arrays exhibit better antireflective performance than 2D arrays over most wavelengths from 400 to 2400 nm. The proposed method not only simplifies the conventional process but also achieves excellent antireflective performance. Hence, this approach may provide potential applications in solar cells, light sensors, LEDs, and other optical devices.

ASSOCIATED CONTENT

Supporting Information

Large-area SEM images of the hierarchical 3D NOA-63 arrays. This material is available free of charge via the Internet at http://pubs.acs.org.

AUTHOR INFORMATION

Corresponding Author

*E-mail: luenan@jlu.edu.cn. Tel/Fax: +86-431-85168477.

Notes

The authors declare no competing financial interest.

ACKNOWLEDGMENTS

We gratefully acknowledge the National Natural Science Foundation of China (No. 21273092) and the National Basic Research Program of China (No. 2009CB939701).

REFERENCES

(1) Ji, S.; Park, J.; Lim, H. *Nanoscale* **2012**, *4*, 4603−4610.
(2) Wei, W. R.; Tsai, M. L.; Ho, S. T.; Tai, S. H.; Ho, C. R.; Tsai, S. H.; Liu, C. W.; Chung, R. J.; He, J. H. *Nano Lett.* **2013**, *13*, 3658−3663.
(3) Lee, C.; Bae, S. Y.; Mobasser, S.; Manohara, H. *Nano Lett.* **2005**, *5*, 2438−2442.
(4) Lee, J. Y.; Connor, S. T.; Cui, Y.; Peumans, P. *Nano Lett.* **2008**, *8*, 689−692.
(5) Liu, K. S.; Yao, X.; Jiang, L. *Chem. Soc. Rev.* **2010**, *39*, 3240−3255.
(6) Watson, G. S.; Watson, J. A. *Appl. Surf. Sci.* **2004**, *235*, 139−144.
(7) Hadobas, K.; Kirsch, S.; Carl, A.; Acet, M.; Wassermann, E. F. *Nanotechnology* **2000**, *11*, 161−164.
(8) Aydin, C.; Zaslavsky, A.; Sonek, G. J.; Goldstein, J. *Appl. Phys. Lett.* **2002**, *80*, 2242−2244.

(9) Sai, H.; Fujii, H.; Arafune, K.; Ohshita, Y.; Yamaguchi, M.; Kanamori, Y.; Yugami, H. *Appl. Phys. Lett.* **2006**, *88*, 201116-1−201116-3.
(10) Sun, C. H.; Min, W. L.; Linn, N. C.; Jiang, P.; Jiang, B. *Appl. Phys. Lett.* **2007**, *91*, 231105-1−231105-3.
(11) Chuang, S. Y.; Chen, H. L.; Shieh, J.; Lin, C. H.; Cheng, C. C.; Liu, H. W.; Yu, C. C. *Nanoscale* **2010**, *2*, 799−805.
(12) Li, X. A.; Xue, L. J.; Han, Y. C. *J. Mater. Chem.* **2011**, *21*, 5817−5826.
(13) Li, X.; Han, Y. C. *J. Mater. Chem.* **2011**, *21*, 18024−18033.
(14) Li, Y. F.; Zhang, J. H.; Yang, B. *Nano Today* **2010**, *5*, 117−127.
(15) Gao, X. F.; Yan, X.; Yao, X.; Xu, L.; Zhang, K.; Zhang, J. H.; Yang, B.; Jiang, L. *Adv. Mater.* **2007**, *19*, 2213−2217.
(16) Cai, W. P.; Li, Y.; Duan, G. T. *J. Adhes. Sci. Technol.* **2008**, *22*, 1949−1965.
(17) Chen, X.; Sun, Z. Q.; Zheng, L. L.; Chen, Z. M.; Wang, Y. F.; Fu, N.; Zhang, K.; Yan, X.; Liu, H.; Jiang, L.; Yang, B. *Adv. Mater.* **2004**, *16*, 1632−1636.
(18) Yan, X.; Yao, J. M.; Lu, G. A.; Chen, X.; Zhang, K.; Yang, B. *J. Am. Chem. Soc.* **2004**, *126*, 10510−10511.
(19) Zhang, J. H.; Yang, B. *Adv. Funct. Mater.* **2010**, *20*, 3411−3424.
(20) Cavallini, M.; Gentili, D.; Greco, P.; Valle, F.; Biscarini, F. *Nat. Protoc.* **2012**, *7*, 1668−1676.
(21) Cavallini, M.; Simeone, F. C.; Borgatti, F.; Albonetti, C.; Morandi, V.; Sangregorio, C.; Innocenti, C.; Pineider, F.; Annese, E.; Panaccione, G.; Pasquali, L. *Nanoscale* **2010**, *2*, 2069−2072.
(22) Shi, G.; Lu, N.; Xu, H. B.; Wang, Y. D.; Shi, S. L.; Li, H.; Li, Y.; Chi, L. F. *J. Colloid Interface Sci.* **2012**, *368*, 655−659.
(23) Liz-Marzán, L. M.; Giersig, M. *Low-Dimensional Systems: Theory, Preparation, and Some Applications*; Kluwer Academic Publishers: Dordrecht, The Netherlands, 2003; p 163.
(24) Xu, H. B.; Lu, N.; Shi, G.; Qi, D. P.; Yang, B. J.; Li, H. B.; Xu, W. Q.; Chi, L. F. *Langmuir* **2011**, *27*, 4963−4967.
(25) Xu, M. J.; Lu, N.; Xu, H. B.; Qi, D. P.; Wang, Y. D.; Chi, L. F. *Langmuir* **2009**, *25*, 11216−11220.
(26) Wu, H. K.; Odom, T. W.; Whitesides, G. M. *J. Am. Chem. Soc.* **2002**, *124*, 7288−7289.
(27) Li, L.; Zhai, T. Y.; Zeng, H. B.; Fang, X. S.; Bando, Y.; Golberg, D. *J. Mater. Chem.* **2011**, *21*, 40−56.
(28) Ono, Y.; Kimura, Y.; Ohta, Y.; Nishida, N. *Appl. Opt.* **1987**, *26*, 1142−1146.
(29) Xu, H. B.; Lu, N.; Qi, D. P.; Hao, J. Y.; Gao, L. G.; Zhang, B.; Chi, L. F. *Small* **2008**, *4*, 1972−1975.
(30) Zhao, Y.; Wang, J. S.; Mao, G. Z. *Opt. Lett.* **2005**, *30*, 1885−1887.
(31) Wang, S.; Yu, X. Z.; Fan, H. T. *Appl. Phys. Lett.* **2007**, *91*, 061105-1−061105-3.
(32) Zhong, J.; Chen, H.; Saraf, G.; Lu, Y.; Choi, C. K.; Song, J. J.; Mackie, D. M.; Shen, H. *Appl. Phys. Lett.* **2007**, *90*, 203515-1−203515-3.
(33) Huang, Y. F.; Chattopadhyay, S.; Jen, Y. J.; Peng, C. Y.; Liu, T. A.; Hsu, Y. K.; Pan, C. L.; Lo, H. C.; Hsu, C. H.; Chang, Y. H.; Lee, C. S.; Chen, K. H.; Chen, L. C. *Nat. Nanotechnol.* **2007**, *2*, 770−774.